Protective effect of necrosulfonamide on rat pulmonary ischemia-reperfusion injury via inhibition of necroptosis

Satoshi Ueda, MD,[a] Toyofumi F. Chen-Yoshikawa, MD, PhD,[b] Satona Tanaka, MD, PhD,[a] Yoshito Yamada, MD, PhD,[a] Daisuke Nakajima, MD, PhD,[a] Akihiro Ohsumi, MD, PhD,[a] and Hiroshi Date, MD, PhD[a]

ABSTRACT

Background: Necroptosis plays an important role in cell death during pulmonary ischemia-reperfusion injury (IRI). We hypothesized that therapy with necrosulfonamide (NSA), a mixed-lineage kinase domain-like protein inhibitor, would attenuate lung IRI.

Methods: Rats were assigned at random into the sham operation group (n = 6), vehicle group (n = 8), or NSA group (n = 8). In the NSA and vehicle groups, the animals were heparinized and underwent left thoracotomy, and the left hilum was clamped for 90 minutes, followed by reperfusion for 120 minutes. NSA (0.5 mg/body) and a solvent were administered i.p. in the NSA group and the vehicle group, respectively. The sham group underwent 210 minutes of perfusion without ischemia. After reperfusion, arterial blood gas analysis, physiologic data, lung wet-to-dry weight ratio, histologic changes, and cytokine levels were assessed. Fluorescence double immunostaining was performed to evaluate necroptosis and apoptosis.

Results: Arterial partial pressure of oxygen/fraction of inspired oxygen (PaO_2/FiO_2) was better, dynamic compliance was higher, and mean airway pressure and lung edema were lower in the NSA group compared with the vehicle group. Moreover, in the NSA group, lung injury was significantly alleviated, and the mean number of necroptotic cells (55.3 ± 4.06 vs 78.2 ± 6.87; $P = .024$), but not of apoptotic cells ($P = .084$), was significantly reduced compared with the vehicle group. Interleukin (IL)-1β and IL-6 levels were significantly lower with NSA administration.

Conclusions: In a rat model, our results suggest that NSA may have a potential protective role in lung IRI through the inhibition of necroptosis. (J Thorac Cardiovasc Surg 2022;163:e113-22)

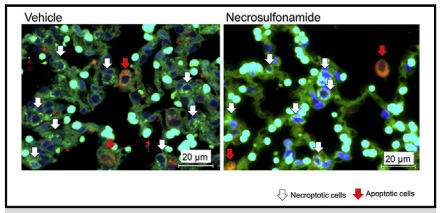

Effect of necrosulfonamide on the number of necroptotic cells and apoptotic cells.

CENTRAL MESSAGE

Necrosulfonamide intervention can produce significant improvements in physiologic function, histologic damage, and attenuation of inflammatory cytokines via the inhibition of necroptosis.

PERSPECTIVE

Necrosulfonamide intervention can produce significant improvements in physiologic function, histologic damage, and attenuation of inflammatory cytokines via the inhibition of necroptosis. The inhibition of necroptosis by a mixed-lineage kinase domain-like protein inhibitor appears to be a promising new option for protective treatment against ischemia-reperfusion injury.

See Commentaries on pages e123 and e124.

Video clip is available online.

Pulmonary disorders characterized by ischemia-reperfusion injury (IRI) are associated with many clinical manifestations, including pulmonary embolism, single-lung ventilation, and lung transplantation, causing alveolar damage, pulmonary edema, and infiltration of inflammatory cells.[1-3] Regarding the relationship between IRI and cell death, resultant cell death has morphologic features of necrosis. However, programmed or regulated cell death was considered synonymous with apoptosis until pathways of regulated necrosis were described.[4,5] Because necrosis was considered unregulated and uncontrollable, few studies have been performed on the mechanism regulating necrosis in IRI.

From the [a]Department of Thoracic Surgery, Kyoto University Graduate School of Medicine, Kyoto, Japan and [b]Department of Thoracic Surgery, Nagoya University Graduate School of Medicine, Nagoya, Japan.

Received for publication Sept 30, 2020; revisions received Dec 22, 2020; accepted for publication Jan 10, 2021; available ahead of print Jan 22, 2021.

Address for reprints: Hiroshi Date, MD, PhD, Department of Thoracic Surgery, Kyoto University Graduate School of Medicine, 54 Shogoin Kawahara-cho, Sakyo-ku, Kyoto 606-8507, Japan (E-mail: hdate@kuhp.kyoto-u.ac.jp).

0022-5223/$36.00

https://doi.org/10.1016/j.jtcvs.2021.01.037

Abbreviations and Acronyms

DAMP = damage-associated molecular pattern
DAPI = 4′,6-diamidino-2-phenylindole
DMSO = dimethyl sulfoxide
ELISA = enzyme-linked immunoassay
HMGB1 = high-mobility group box protein 1
HPF = high-power field
IL = interleukin
IRI = ischemia-reperfusion injury
MLKL = mixed-lineage kinase domain-like protein
Nec-1 = necrostatin-1
NSA = necrosulfonamide
RIPK1 = receptor-interacting protein kinase-1
RIPK3 = receptor-interacting protein kinase-3
TNF-α = tumor necrosis factor alpha
TUNEL = terminal deoxynucleotidyl transferase-dUTP nick-end labeling
TV = tidal volume

This consensus has recently changed dramatically after the discovery of signaling pathways inducing regulated necrosis.[4-6] The best-characterized regulated necrosis is necroptosis, which is a form of cell death controlled by death signals and displays a death pattern like that of necrosis.[4,5] Different from apoptosis, necroptosis is a caspase-independent regulated type of cell death that depends on the stream of cellular signals, which is composed mainly of the receptor-interacting protein kinase-1 (RIPK1), receptor-interacting protein kinase-3 (RIPK3), and mixed-lineage kinase domain-like protein (MLKL)[5,7-9] (Figure 1). The mechanistic pathway controlled by the activation of these molecules plays a pivotal role in necroptosis.

Recent studies suggest that necroptosis has a pathologic and physiologic role in clinical pulmonary diseases in IRI,[10,11] chronic obstructive pulmonary disease,[12] lung cancer,[13] and sepsis.[14] It has been reported that RIPK1 inhibitor necrostatin-1 (Nec-1) can decrease the activation of necroptosis via the inhibition of necroptosis in several clinical IRI-based studies.[7,10,15-18] On the other hand, it also has been reported that in a mouse tumor necrosis factor alpha (TNF-α)-mediated shock model (a mimic model of IRI), Nec-1 failed to protect but further accelerated time to death.[5,19] According to those reports, it was also demonstrated that RIPK3-deficient mice were markedly protected from TNF-α–mediated shock, indicating that the inhibition of necroptosis would be performed at the level of RIPK3 or further downstream molecules.[20] Consequently, RIPK3 and further downstream molecules were considered to generate the key signals in the regulated necrosis pathway, and MLKL and necrosulfonamide (NSA [(E)-N-(4-(N-(3-methoxypyrazin-2-yl)sulfamoyl)phenyl)-3-(5-nitrothiophene-2-yl)acrylamide]),

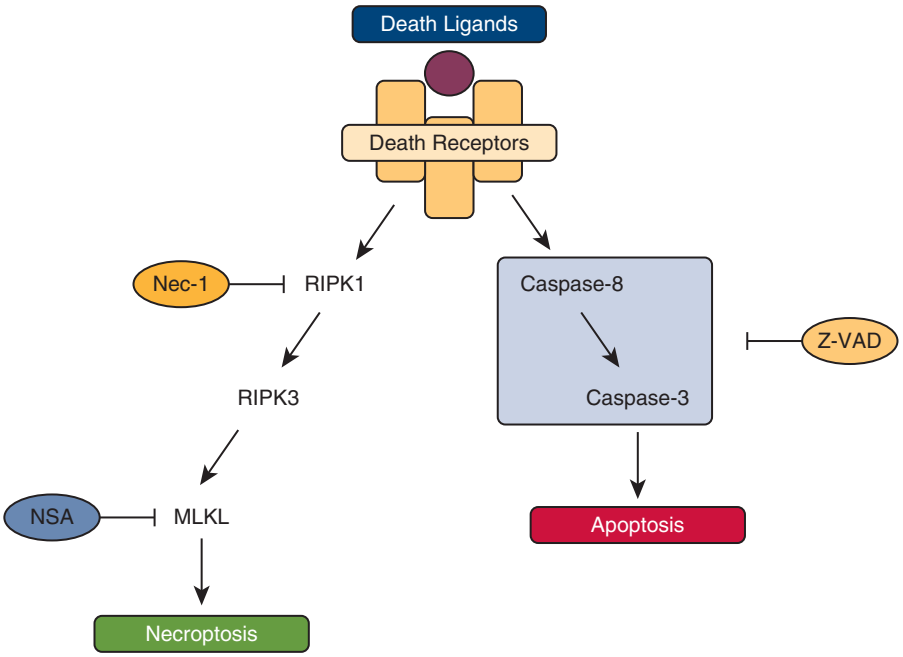

FIGURE 1. Outline of major molecules and inhibitors in regulated cell death. Cell death caused by the engagement of pathways that lead to the activation of caspase proteases presents with the morphologic features of apoptosis. The activation of caspase is suppressed by Z-Val-Ala-DL-Asp-Asp-fluoromethylketone (*Z-VAD*). On the other hand, necroptosis is a caspase-independent regulated type of cell death depending on the stream of cellular signals, which is composed mainly of the receptor-interacting protein kinase-1 (*RIPK1*), receptor-interacting protein kinase-3 (*RIPK3*), and mixed-lineage kinase domain-like protein (*MLKL*). Necrostatin-1 (*Nec-1*) and necrosulfonamide (*NSA*) inhibit necroptosis by inhibiting RIPK1 and MLKL, respectively.

an inhibitor of MLKL, were considered critically relevant.[20] However, because NSA is a relatively new drug, there have been few reports on its administration, especially in IRI attenuation.

We hypothesized that the NSA administration might play an important role in alleviating lung IRI via the inhibition of necroptosis. To verify this hypothesis, we conducted a small animal study using a rat lung IRI model.

METHODS

Animals

The experiments were done on 22 male Lewis rats weighing 280-320 g (Japan SLC, Hamamatsu, Japan). All animals received humane care in compliance with the Principles of Laboratory Animal Care formulated by the National Society for Medical Research. All experimental protocols received approval from the Ethics Committee of the Graduate School of Medicine at Kyoto University.

Rat Hilar Clamp Model to Evaluate Cell Death and IRI

Rats were assigned at random into 3 groups: sham group (n = 6), vehicle group (n = 8), and NSA group (n = 8). Rats in the sham operation group did not receive other procedures except for thoracotomy (left lung) and 210-minute ventilation. Figure 2 shows the outline of the experimental method. Anesthesia was induced inhalation of isoflurane, followed by intraperitoneal injection of sodium pentobarbital (100 mg/kg). Heparin (1000 U/kg) was initially administered subcutaneously. NSA (0.5 mg) was dissolved with 0.5 mL of 20% dimethyl sulfoxide (DMSO) and injected intraperitoneally in the NSA group,[21,22] while 0.5 mL of 20% DMSO without NSA was administered in the vehicle group. After tracheostomy and incubation with a plastic catheter, mechanical ventilation was started (Model SN-480-7; Shinano Seisakujo, Tokyo, Japan). Throughout the experiment, the fraction of inspired oxygen was kept at 100%, and positive end-expiratory pressure was maintained at 2 cm H_2O. During bilateral lung ventilation, we set the tidal volume (TV) to 9 mL/kg and the respiratory rate to 60 breaths/minute. Left thoracotomy was performed, and the left hilum was occluded with a small metallic clamp for 90 minutes. Occlusion was performed 30 minutes after the administration of NSA or vehicle, at which point the TV was reduced to 6 mL/kg until reperfusion. After 90 minutes of occlusion, the clamp was released, and reperfusion was performed by restoring blood flow and ventilation to the bilateral lung.

Arterial Blood Gas Analysis and Lung Mechanics Outcome Measures

Lung injury was assessed using a median sternotomy to occlude the right hilum (including the accessory lobe) after 120 minutes of reperfusion. The TV and respiratory rate were set to 5 mL/kg and 60 breaths/minute, respectively. After 5 minutes, a blood sample was collected through the ascending aorta for arterial blood gas analysis. The animals were then connected to the flexiVent system (SCIREQ, Montreal, Canada). Physiologic data, dynamic compliance, mean airway pressure, and peak airway pressure were measured by alternating perturbations of the single forced oscillation families in a closely spaced manner (Snap-Shot; SCIREQ).

Lung Wet-to-Dry Weight Ratio

The upper part of the left lung was used to calculate the lung wet-to-dry weight ratio, as reported previously.[1,2,23] The wet weight was measured soon after the harvest, and the dry weight was measured after drying at 100°C for 24 hours. The ratio was calculated as wet weight divided by dry weight.

Histologic Analysis

The middle left lung was fixed in 10% formalin and stained with hematoxylin and eosin. For quantitative histologic evaluation of ischemia reperfusion injury, vascular edema, extravascular red blood cell count, and alveolar or interstitial neutrophil infiltration were determined, as described

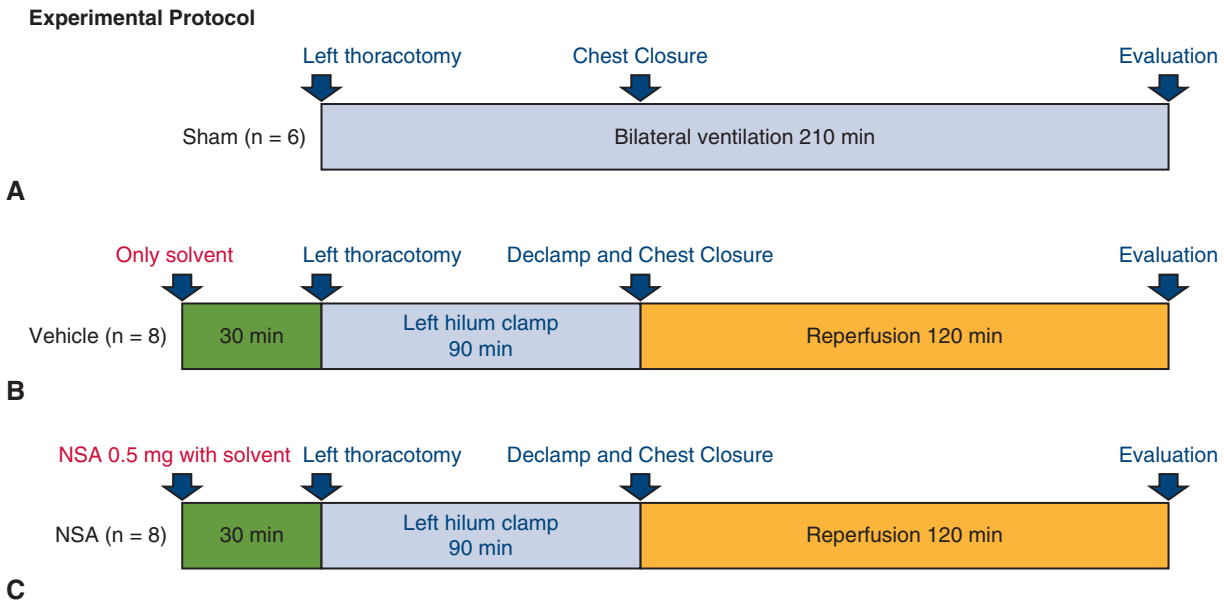

FIGURE 2. Diagram of the experimental protocol. Three experiments were performed, with rats assigned at random to the sham group (n = 6) (A), vehicle group (n = 8) (B), or necrosulfonamide (*NSA*) group (n = 8) (C). In the NSA and vehicle groups, rats were heparinized and underwent left thoracotomy, and the left hilum was clamped for 90 minutes, followed by reperfusion for 120 minutes. NSA (1.65 mg/kg) and a solvent were administered intraperitoneally in the NSA group and the vehicle group, respectively. The sham group underwent 210 minutes of perfusion without ischemia.

previously.[1,2] The perivascular cuff area was measured in 5 randomly chosen vessels per section at a magnification of 200×. The ratio of perivascular cuff area to vessel area was calculated automatically with BZ-H4C software (Keyence, Osaka, Japan), as described previously.[24] Red blood cell and neutrophil counts were expressed by the average number in 10 randomly chosen high-power fields (HPFs; 400× magnification) per section. Cell counting was also done automatically using BZ-H4C software.[24] To get the BZ-H4C software to properly recognize neutrophils infiltrating into the perivascular area, in addition to hematoxylin and eosin, naphthol AS-D chloroacetate esterase stain was used secondarily.

Western Blot Analysis

The lower part of the left lung, which had been stored at −80°C, was suspended in an ice-cold radioimmunoprecipitation assay buffer containing a cocktail of protease and phosphatase inhibitors (Nacalai Tesque, Kyoto, Japan), and centrifuged at 13,000× *g* for 10 minutes, as reported previously.[23] The protein concentration was determined by a Bradford protein assay and adjusted evenly. The protein samples (15 μg) were loaded on sodium dodecyl sulfate–polyacrylamide gels for electrophoresis and transferred to a PVDF membrane. The membrane was incubated with primary and secondary antibodies using standard procedures and visualized with the EzWestLumi Plus Detection Kit (Atto, Tokyo, Japan), with detection of luminescence using the LuminoGraph II imaging system (Atto).[25] The same membrane was used for repeated probing for β-actin, which was used as an internal loading control. Band densitometry analysis was performed using ImageJ version 1.52s.

Immunofluorescence Staining for Lung Necroptosis or Apoptosis

Immunofluorescence double staining of terminal deoxynucleotidyl transferase-dUTP nick-end labeling (TUNEL) and caspase-3 cells was conducted to determine necrotic/apoptotic cells, as described previously.[26] For double labeling with cleaved caspase-3, after TUNEL staining, DAPI (4′,6-diamidino-2-phenylindole) was used to stain the nuclei. Immunofluorescence reactivity visualization was performed on a fluorescence microscope (BZ-X800; Keyence), depicting 10 randomly chosen HPFs per section. Necroptotic and apoptotic cells counting was automatically performed using the BZ-H4C software.[24] Necroptosis and apoptosis cells were counted by having the BZ-H4C software first recognize the cell nuclei, which are stained with DAPI, and then discriminating the cytoplasmic color of the cells, respectively.

Enzyme-Linked Immunosorbent Assay

The same quantities of the 10 mg lower left lung were homogenized with 500 μL of phosphate-buffered saline with protease inhibitors (Wako, Osaka, Japan) and then centrifuged (10,000× *g* for 20 minutes) to obtain tissue lysates of lung to perform an enzyme-linked immunosorbent assay (ELISA). The concentrations of TNF-α, interleukin (IL)-1β, and IL-6 in tissue lysates of lung were measured using ELISA kits following the manufacturer's instructions.

Reagents and Antibodies

NSA was provided by Bio Vision (Milpitas, Calif). The dose of 0.5 mg/body and intraperitoneal administration were adopted based on previous reports.[21,22] Chemicals of highest purity available were used. The following antibodies were used: anti-MLKL (Biorbyt, Cambridge, United Kingdom), anti-RIPK1 (Novus Biologicals, Littleton, Colo), anti-RIPK3 (Enzo Life Sciences, Lörrach, Germany), anti–high-mobility group box protein 1 (HMGB1; GeneTex, Irvine, Calif), cleaved caspase-3 (Cell Signaling Technology, Danvers, Mass), and β-actin (A5441; Sigma-Aldrich, St Louis, Mo). Rat ELISA kits used in this experiment included TNF-α (Novus), IL-6 (R&D Systems, Minneapolis, Minn), and IL-1β (Immuno-Biological Laboratories, Gunma, Japan).

Statistical Analysis

Data are presented as the mean ± standard error of the mean. Comparisons between 2 independent groups were performed using the Mann–Whitney *U* test. All statistical analyses were performed with JMP pro 14.0 (SAS Institute, Cary, NC), with $P < .05$ considered to indicate statistical significance.

RESULTS

Effect of NSA on Lung Function and Wet-to-Dry Weight Ratio

Arterial oxygenation (Figure 3, *A*) and dynamic compliance (Figure 3, *B*) were higher in the NSA group compared with the vehicle group (379 ± 31.9 mmHg vs 269 ± 21.4 mmHg [$P = .0009$] and 0.141 ± 0.012 mL/cmH_2O vs 0.122 ± 0.0166 mL/cmH_2O [$P = .036$], respectively). Maximum and mean airway pressures were lower in the NSA group (22.4 ± 1.37 cmH_2O vs 26.1 ± 2.86 cmH_2O [$P = .018$] and 10.1 ± 0.94 cmH_2O vs 11.6 ± 1.35 cmH_2O [$P = .039$], respectively) (Figure 3, *C* and *D*). Lung edema (wet-to-dry weight ratio) was significantly reduced in the NSA group relative to the vehicle group (4.92 ± 0.53 vs 5.99 ± 0.723; $P = .014$) (Figure 3, *E*).

Histologic Effect of NSA

The NSA group showed a significantly lower average number of extravascular red blood cells per section at a magnification of 400× compared with the vehicle group (622 ± 66.6 per HPF vs 792 ± 65.7 per HPF; $P = .041$) (Figure 4, *D*). The number of neutrophil infiltrations into the perivascular area was markedly reduced in the NSA group compared with the vehicle group (20 ± 9.64 per HPF vs 41.5 ± 14.8 per HPF; $P = .018$) (Figure 4, *E*). The perivascular cuff area was measured in 5 vessels per histologic section, which resulted in 30 vessels for the sham group and 40 vessels for both the vehicle and NSA groups. We calculated the index of perivascular cuff area to the vessel area to eliminate variations related to vessel size. The index was significantly lower in the NSA group (0.934 ± 0.212 vs 1.82 ± 0.43; $P = .0009$) (Figure 4, *F*).

Expression of Necroptosis-Associated Target Molecules

Western blot analysis showed a significantly reduced MLKL/β-actin level in the NSA group ($P = .037$) (Figure 5, *A*). NSA administration did not reduce the levels of RIPK1 and RIPK3 ($P = .11$) (Figure 5, *B* and *C*). The expression level of HMGB1 released by cell death was significantly lower in the NSA group compared with the vehicle group ($P = .045$) (Figure 5, *D*).

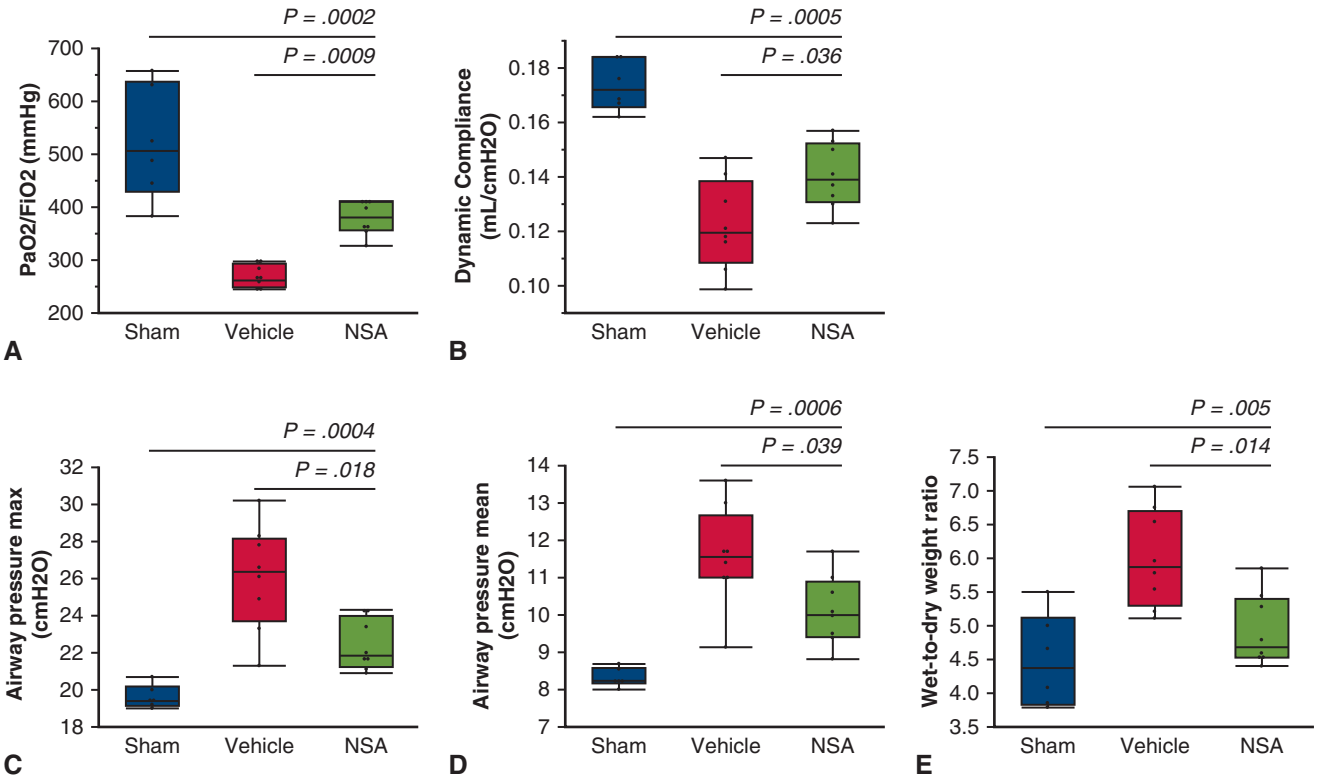

FIGURE 3. Pulmonary function of the left lungs: arterial partial pressure of oxygen/fractional inspired oxygen (PaO_2/FiO_2) (A), dynamic pulmonary compliance (B), peak airway pressure (C), mean airway pressure (D), and wet-to-dry weight ratio (E). All parameters were significantly improved in the necrosulfonamide (*NSA*) group relative to the vehicle group. In the graphs, the *upper* and *lower borders* of the box represent the upper and lower quartiles; the *upper* and *lower whiskers* represent the maximum and minimum values of nonoutliers, and the *middle horizontal line* represents the median. Data are presented as mean ± standard error of the mean. Multiple comparisons among the groups were performed using the Kruskal–Wallis test. The comparison between 2 independent groups was performed using the Mann–Whitney *U* test. All statistical analyses were performed with JMP pro 14.0 (SAS Institute, Cary, NC), with $P < .05$ considered to indicate statistical significance.

Necroptotic Cells or Apoptotic Cells

Immunofluorescence revealed that necroptotic cells (positive only for TUNEL) were stained green in the cytoplasm, whereas apoptotic cells (positive for both TUNEL and caspase-3) were stained red to yellow in the cytoplasm (Figure 6). In addition, the mean number of necroptotic cells was significantly lower in the NSA group compared with the vehicle group (55.3 ± 11.5 per HPF vs 78.2 ± 19.4 per HPF; $P = .024$) (Figure 7, *A*). NSA administration did not significantly reduce the mean number of apoptotic cells compared with the vehicle group (4.86 ± 2.85 per HPF vs 12.8 ± 10.7 per HPF; $P = .083$) (Figure 7, *B*). Finally, in each group, the average number of necroptotic cells was significantly higher than that of apoptotic cells.

Effect of NSA on Cytokine Levels

TNF-α levels were not significantly lower in the NSA group compared with the vehicle group (535 ± 41.4 pg/mL vs 607 ± 104 pg/mL; $P = .25$) (Figure 8, *A*), whereas the levels of both IL-1β and IL-6 were significantly lower relative to the vehicle group (1681 ± 340 pg/mL vs 1313 ± 265 pg/mL [$P = .021$] and 269 ± 73.1 pg/mL vs 409 ± 126 pg/mL [$P = .036$], respectively) (Figure 8, *B* and *C*).

DISCUSSION

This study demonstrates that the administration of NSA significantly improved lung IRI via the inhibition of necroptosis in a simple and validated in vivo model. Our data show that in damaged lungs, physiologic functions were significantly improved by NSA administration. Pathologic findings of the hemorrhagic area and neutrophil infiltration were significantly attenuated in the NSA group. Perivascular edema, evaluated by the wet-to-dry weight ratio and vascular cuff, was ameliorated in the NSA group. Western blot analysis also indicated that NSA can precisely inhibit the MLKL. In addition, fluorescent double immunostaining made it possible to visualize and perform a quantitative evaluation in the damaged lungs, which allowed us to evaluate necroptosis and apoptosis individually. To our knowledge, this is the first report exploring the potential

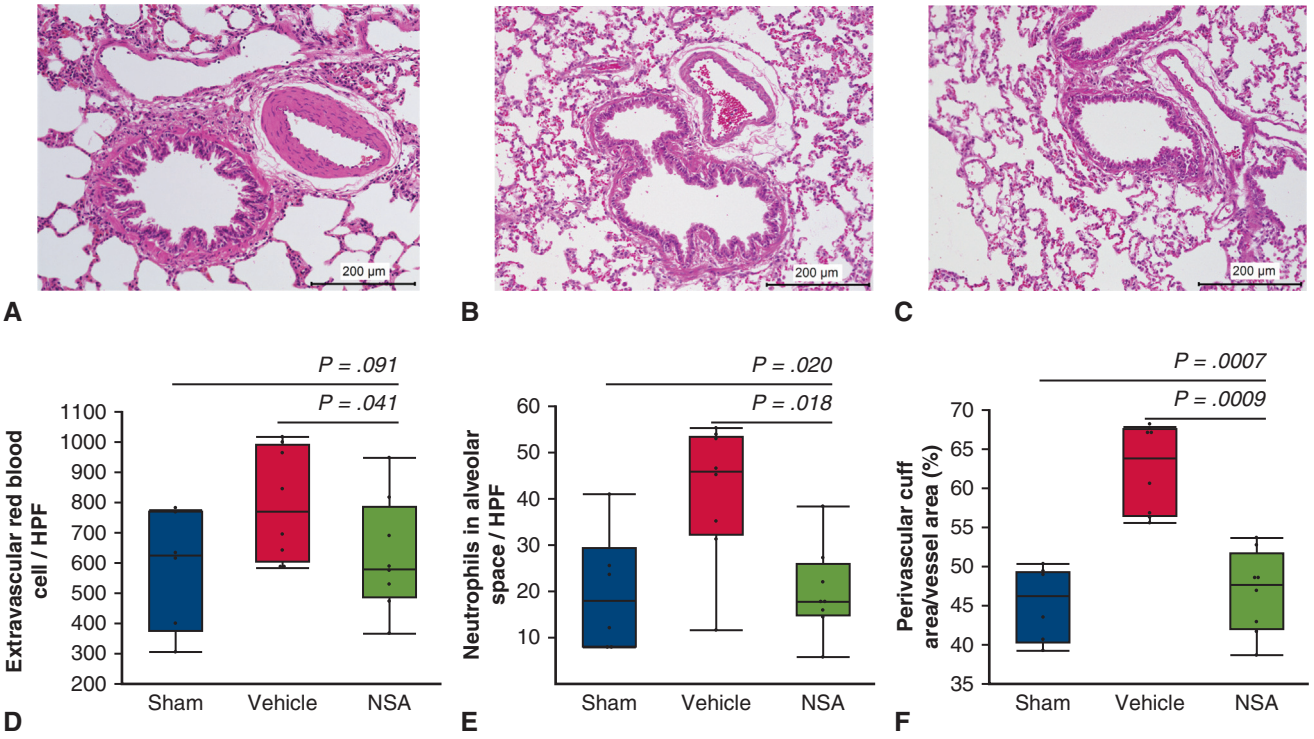

FIGURE 4. Hematoxylin and eosin stain analysis (original magnification 200×). (A–C) Representative histologic section of the left lungs of sham group (A), vehicle group (B), and necrosulfonamide (*NSA*) group (C). (D and E) The average number counted of both extravascular red blood cells (D) and neutrophils (E) in the alveolar or interstitial space was significantly lower in the NSA group. (F) Perivascular edema evaluated using vascular cuff was also ameliorated in the NSA group. In the graphs, the *upper* and *lower borders* of the box represent the upper and lower quartiles. The *upper* and *lower whiskers* represent the maximum and minimum values of nonoutliers. The *middle horizontal line* represents the median. Data are presented as mean ± standard error of the mean. Multiple comparisons among the groups were performed using the Kruskal–Wallis test. Comparisons between 2 independent groups were performed using the Mann–Whitney *U* test. All statistical analyses were performed with JMP pro 14.0 (SAS Institute, Cary, NC), and $P < .05$ was considered to indicate statistically significance. *HPF*, High-power field.

protective effect of NSA treatment on lung IRI, and on the visual evaluation of the cell death in damaged lungs using fluorescent double immunostaining.

NSA is known to specifically block necroptosis downstream of RIPK3 activation.[20] As the interacting target of NSA, MLKL was also revealed, because a specific step at which RIPK3 formed discrete punctate in cells was arrested by treating the cells with NSA or knocking down MLKL expression.[20] MLKL has been considered one of the key RIPK3 downstream components in IRI[8,27]; therefore, we focused on MLKL as a RIPK3 peripheral molecule in necroptosis downstream of RIPK1 and performed the intervention with NSA. As for the studies based on NSA, previous reports have shown that NSA attenuated spinal cord injury[21] or that NSA had a protective effect on intestinal epithelial cells via the inhibition of necroptosis.[26] However, there have been few reports on IRI attenuation due to NSA administration, other than 2017 study showing that NSA improved neurologic function after IRI.[28] Therefore, we consider the present study worthwhile for its evaluation of IRI attenuation in solid organs due to intervention with NSA.

It has been assumed that necroptosis emerges as an instrument of innate immunity during infectious diseases and is a protective mode of cell death that eliminates pathogen-infected cells.[5,29] However, for diseases involved in inflammatory processes, including IRI, atherosclerosis, sepsis, inflammatory bowel disease, neurodegenerative diseases, and autoimmune diseases, the necroptosis pathway can do harm rather than contribute to protection. This idea may be supported by the fact that, different from apoptosis, the release of cytosolic contents and/or cell death–associated molecular patterns (DAMPs) occurs in necroptotic cells by membrane rupture, and these molecules signal the immune system to tissue damage and induce an inflammatory response.[30,31] Thus, regulated necrosis can substantially influence immunity and organ survival. In the present study, it was also verified by the attenuation of HMGB1, a kind of DAMP, as confirmed by Western blot analysis. In addition, in lung tissue, IL-6 and IL-1β, inflammatory cytokines released by cell rupture or membrane permeabilization,[32,33] also were attenuated with the administration of NSA. Because Western blot analysis indicated that NSA can precisely inhibit MLKL rather than

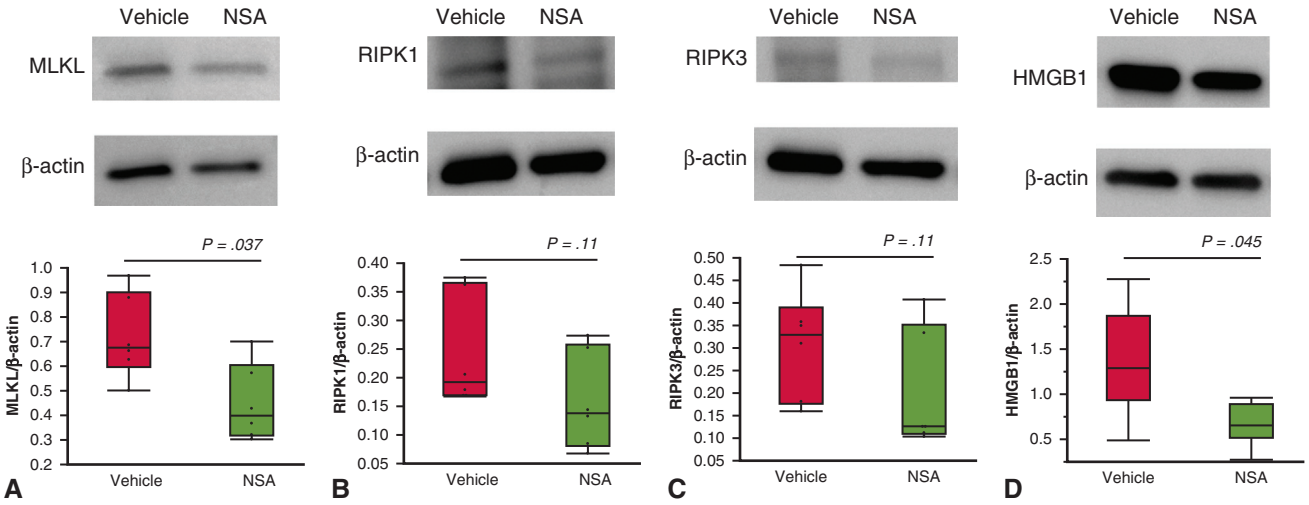

FIGURE 5. Western blot analysis of mixed-lineage kinase domain-like protein (*MLKL*) (A), receptor-interacting protein kinase-1 (*RIPK1*) (B), receptor-interacting protein kinase-3 (*RIPK3*) (C), and high-mobility group box protein 1 (*HMGB1*) (D) in lung tissue lysates of the necrosulfonamide (*NSA*) group and the vehicle group. Band densitometry analysis was performed using ImageJ. β-actin expression served as an internal loading control. MLKL ($P = .037$) and HMGB1 ($P = .045$) were significantly reduced in the NSA group compared with the vehicle group. In the graphs, the *upper* and *lower borders* of the box represent the upper and lower quartiles, the *upper* and *lower whiskers* represent the maximum and minimum values of nonoutliers, and the *middle horizontal line* represents the median. Data were presented as mean ± standard error of the mean. Comparisons between 2 independent groups were performed using the Mann–Whitney *U* test. All statistical analyses were performed with JMP pro 14.0 (SAS Institute, Cary, NC), with $P < .05$ considered to indicate statistical significance.

RIPK1 and RIPK3, the inhibition of MLKL may be considered to attenuate the release of cytosolic contents. The fact that extracellular release of inflammatory cytokines can promote adaptive immune responses suggests that NSA can indirectly inhibit the spread of inflammation along with inhibiting necroptosis.

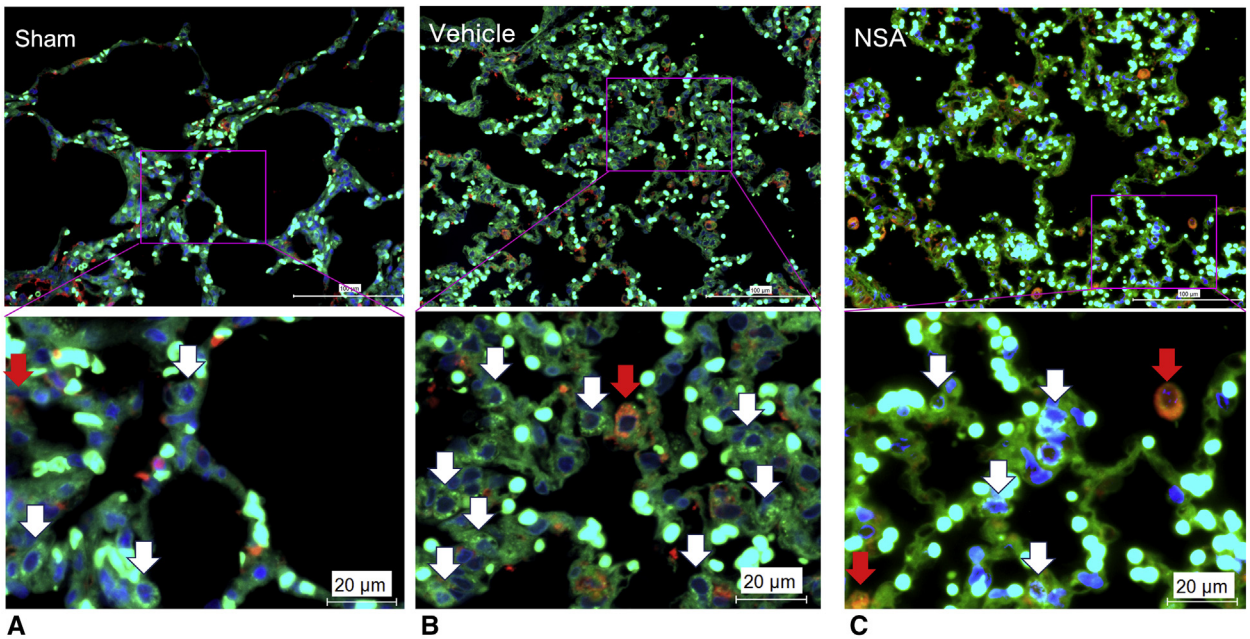

FIGURE 6. Analysis of immunofluorescence double staining with terminal deoxynucleotidyl transferase-dUTP nick-end labeling (TUNEL) and caspase-3 cells in the sham group (A), vehicle group (B), and necrosulfonamide (*NSA*) group (C) (Original magnification 200× and 400×.) TUNEL-positive and caspase-3–negative cells were counted as necroptotic cells (*white arrows*), and TUNEL-positive and caspase-3–positive were counted as apoptotic cells (*red arrows*).

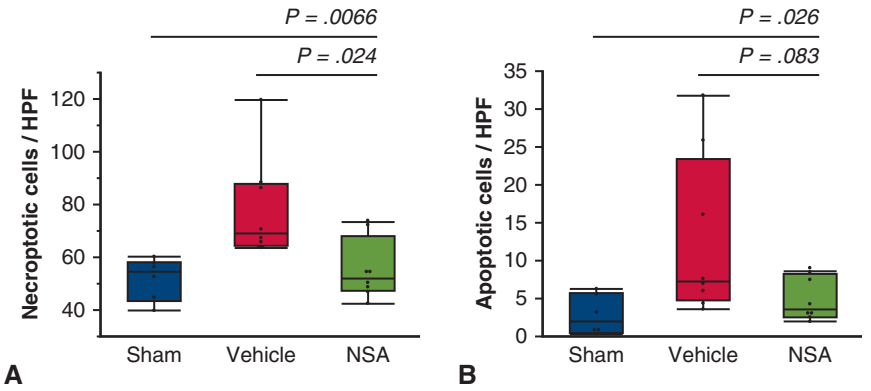

FIGURE 7. Average numbers of necroptotic cells and apoptotic cells were counted using a fluorescence microscope (BZ-X800; Keyence). Necroptotic cells were significantly reduced in the necrosulfonamide (*NSA*) group compared with the vehicle group ($P = .024$) (A); however, NSA administration did not significantly reduce the number of apoptotic cells compared with the vehicle group ($P = .083$) (B). Also, in each group, the average number of necroptotic cells was significantly higher than that of apoptotic cells. In the graphs, the *upper* and *lower borders* of the box represent the upper and lower quartiles, the *upper* and *lower whiskers* represent the maximum and minimum values of nonoutliers, and the *middle horizontal line* represents the median. Data are presented as mean ± standard error of the mean. Multiple comparisons among the groups were performed using by the Kruskal–Wallis test. Comparisons between 2 independent groups were performed using the Mann–Whitney *U* test. All statistical analyses were performed with JMP pro 14.0 (SAS Institute), with $P < .05$ considered to indicate statistical significance. *HPF*, High-power field.

It was also reported that in a mouse kidney IRI model, the protective effect disappeared almost completely when Nec-1 was applied at 30 min after reperfusion and was strongly reduced when Nec-1 was applied at 15 min following reperfusion.[34] Thus, because reperfusion can release significant amounts of inflammatory cytokines, which may be one of the reasons for necroptotic signaling in IRI, it would be desirable to administer the necroptosis inhibitor as soon as possible to prevent necroptotic signaling in IRI. Ideally, the necroptosis inhibitor should be administered before reperfusion, as was done in this experiment. In our study, although the necroptosis inhibitor was administered before ischemia, significant improvements were seen in the NSA group. However, more detailed data should be obtained in future studies by performing the experiment with drug administration at various times.

Considering the inhibition of necroptosis as regulated cell death itself, the fluorescent double immunostaining revealed significantly reduced levels of necroptotic cells in the NSA group. In this study, the number of necroptotic cells was mildly increased in the sham group, possibly due to the mechanical ventilation and/or stimulation of thoracotomy and chest closure. Considering this, the NSA intervention might precisely reduce the number of necroptotic cells, because the number of necroptotic cells in the sham group and NSA group was similar (51.9 ± 7.95 per HPF vs 55.3 ± 11.5 per HPF; $P = .095$).

In addition, fluorescent immunostaining also revealed that a higher necroptotic cell count compared with apoptotic

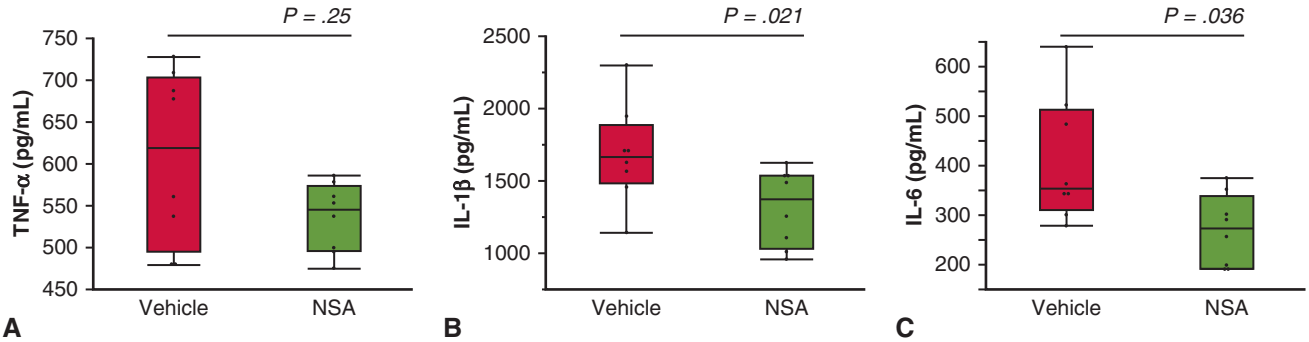

FIGURE 8. Level of tumor necrosis factor-alpha (*TNF-α*) (A), interleukin (*IL*)-1*β* (B), and IL-6 (C) in lung tissue lysates of the 2 groups: vehicle and necrosulfonamide (*NSA*). IL-1*β* and IL-6 levels were significantly lower in the NSA group. In the graphs, the *upper* and *lower borders* of the box represent the upper and lower quartiles, the *upper* and *lower whiskers* represent the maximum and minimum values of nonoutliers, and the *middle horizontal line* represents the median. Data are presented as mean ± standard error of the mean. Comparisons between 2 independent groups were performed using the Mann–Whitney *U* test. All statistical analyses were performed with JMP pro 14.0 (SAS Institute), with $P < .05$ considered to indicate statistical significance.

cell count in this IRI model. It has been reported that during shorter periods of ischemia, the mode of cell death after reperfusion is primarily apoptosis, and that in longer ischemic periods, cell death after reperfusion is predominately necrosis.[6] Thus, increasing levels of necrotic cells, including regulated necrosis, would be associated with a significant deterioration of organ function in IRI.[6,10] Therefore, considering the cell death due to IRI, inhibiting regulated necrosis, including necroptosis, would be the most important action to prevent tissue deterioration and inflammatory cytokines suppression caused by cell rupture.

Several limitations of this study should be noted. As the response of the immune system of rats is different from that of human, it is necessary to confirm our findings in other animal models before applying these results to humans. Also, although it was showed that the enhanced tissue protein level of MLKL induced by IRI was significantly reduced by the NSA intervention, the concentration of NSA in blood samples or lung tissues remains to be confirmed. Furthermore, this study used only a presurgical administration and single dose of NSA (1.65 mg/kg), whereas using variable administration and titration of dosage would provide useful information on the optimal timing and dose. Regarding safety, although it has been reported that no obvious toxicity from NSA administration was detected in rat liver, kidney, heart, and spleen,[21] potential side effects of concern remain to be verified in future studies. In addition, our data suggest that NSA administration might be better timed before necroptotic signaling in IRI. The situations in which the efficacy of necroptosis inhibitor can be expected are limited to a few settings, such as solid organ transplantation, where the drug can be administered before reperfusion. Therefore, further investigations, including in a lung transplantation model, are needed to investigate these issues. To perform a lung transplantation model, we should consider the differences in the ischemic conditions (such as warm ischemia alone or cold ischemia followed by warm ischemia), and the need to consider the response of the immune system caused by using 2 individual lives. Finally, the Western blot analysis and ELISA were performed without a sham group, owing to the limitations of the experimental equipment.

In conclusion, we have demonstrated that the MLKL inhibitor NSA attenuates IRI through inhibition of necroptosis and improvement of lung-damaged function. The NSA intervention was associated with significant improvements in physiologic function, histologic damage, and attenuation of inflammatory cytokines via the inhibition of necroptosis. The inhibition of necroptosis by an MLKL inhibitor might be one of the promising new options for protective treatment against IRI (Figure 9 and Video 1).

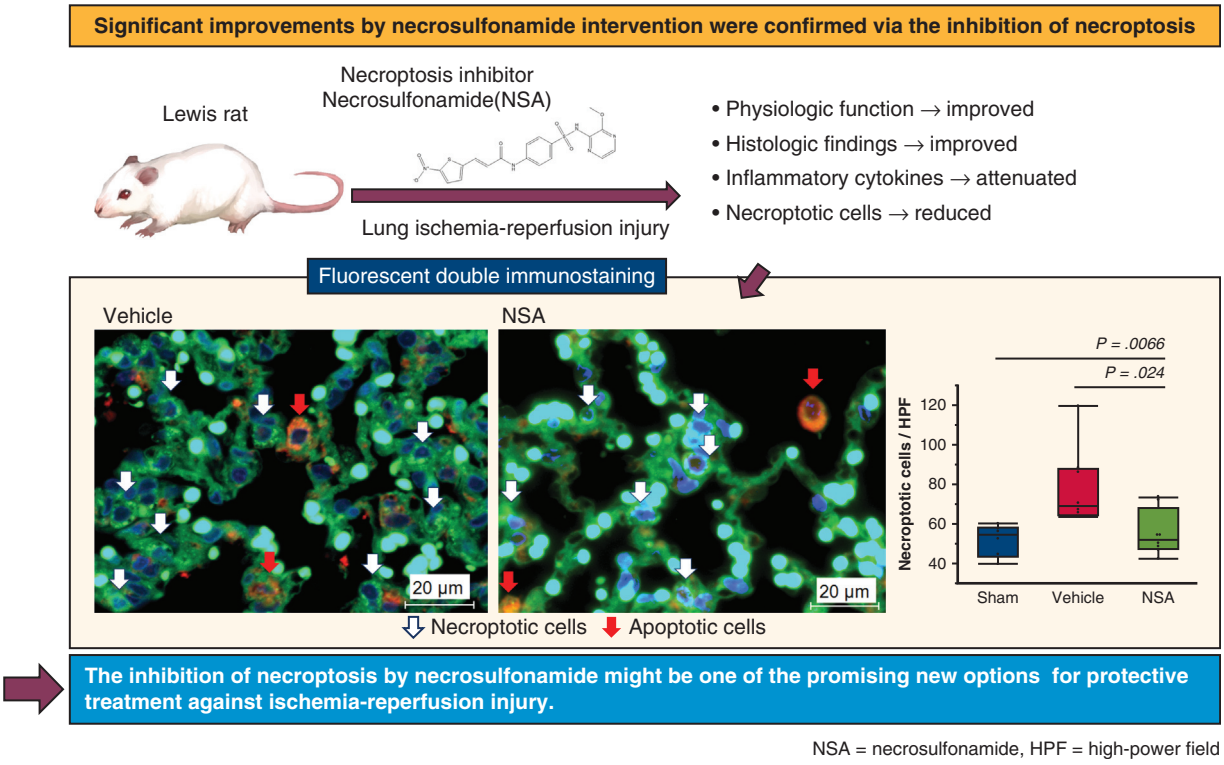

NSA = necrosulfonamide, HPF = high-power field

FIGURE 9. Administration of necrosulfonamide (NSA) significantly improved lung ischemia-reperfusion injury (IRI) via the inhibition of necroptosis in our rat model. Significant improvements in physiologic function, histologic damage, and attenuation of inflammatory cytokines via the inhibition of necroptosis were confirmed. Also, the fluorescent double immunostaining revealed that the necroptotic cells were significantly reduced by the NSA intervention. The inhibition of necroptosis by NSA might be a promising new option for protective treatment against IRI.

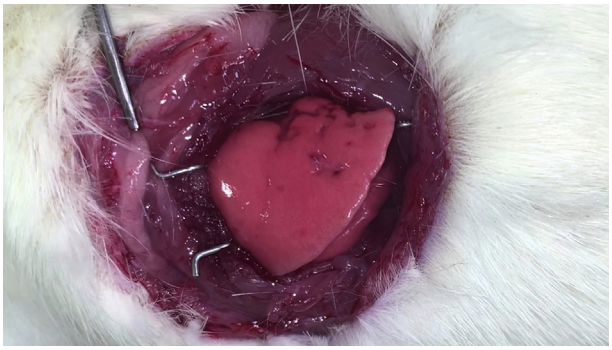

VIDEO 1. Short video showing the experimental procedure and results of this study. Video available at: https://www.jtcvs.org/article/S0022-5223(21)00134-3/fulltext.

Conflict of Interest Statement

The authors reported no conflicts of interest.

The *Journal* policy requires editors and reviewers to disclose conflicts of interest and to decline handling or reviewing manuscripts for which they may have a conflict of interest. The editors and reviewers of this article have no conflicts of interest.

We thank Dr Akihiko Yoshizawa for his advice on pathologic evaluation.

References

1. Saito M, Chen-Yoshikawa TF, Suetsugu K, Okabe R, Takahagi A, Masuda S, et al. Pirfenidone alleviates lung ischemia-reperfusion injury in a rat model. *J Thorac Cardiovasc Surg*. 2019;158:289-96.
2. Tanaka S, Chen-Yoshikawa TF, Kajiwara M, Menju T, Ohata K, Takahashi M, et al. Protective effects of imatinib on ischemia/reperfusion injury in rat lung. *Ann Thorac Surg*. 2016;102:1717-24.
3. Chen F, Date H. Update on ischemia-reperfusion injury in lung transplantation. *Curr Opin Organ Transplant*. 2015;20:515-20.
4. Lau A, Wang S, Jiang J, Haig A, Pavlosky A, Linkermann A, et al. RIPK3-mediated necroptosis promotes donor kidney inflammatory injury and reduces allograft survival. *Am J Transplant*. 2013;13:2805-18.
5. Linkermann A, Green DR. Necroptosis. *N Engl J Med*. 2014;370:455-65.
6. Fischer S, Maclean AA, Liu M, Cardella JA, Slutsky AS, Suga M, et al. Dynamic changes in apoptotic and necrotic cell death correlate with severity of ischemia-reperfusion injury in lung transplantation. *Am J Respir Crit Care Med*. 2000;162:1932-9.
7. Linkermann A, Hackl MJ, Kunzendorf U, Walczak H, Krautwald S, Jevnikar AM. Necroptosis in immunity and ischemia-reperfusion injury. *Am J Transplant*. 2013;13:2797-804.
8. Zhao J, Jitkaew S, Cai Z, Choksi S, Li Q, Luo J, et al. Mixed lineage kinase domain-like is a key receptor interacting protein 3 downstream component of TNF-induced necrosis. *Proc Natl Acad Sci U S A*. 2012;109:5322-7.
9. Chen S, Lv X, Hu B, Shao Z, Wang B, Ma K, et al. RIPK1/RIPK3/MLKL-mediated necroptosis contributes to compression-induced rat nucleus pulposus cells death. *Apoptosis*. 2017;22:626-38.
10. Kanou T, Ohsumi A, Kim H, Chen M, Bai X, Guan Z, et al. Inhibition of regulated necrosis attenuates receptor-interacting protein kinase 1-mediated ischemia-reperfusion injury after lung transplantation. *J Heart Lung Transplant*. 2018;37:1261-70.
11. Sauler M, Bazan IS, Lee PJ. Cell death in the lung: the apoptosis-necroptosis axis. *Annu Rev Physiol*. 2019;81:375-402.
12. Mizumura K, Cloonan SM, Nakahira K, Bhashyam AR, Cervo M, Kitada T, et al. Mitophagy-dependent necroptosis contributes to the pathogenesis of COPD. *J Clin Invest*. 2014;124:3987-4003.
13. Zec M, Srdic-Rajic T, Krivokuca A, Jankovic R, Todorovic T, Andelkovic K, et al. Novel selenosemicarbazone metal complexes exert anti-tumor effect via alternative, caspase-independent necroptotic cell death. *Med Chem*. 2014;10:759-71.
14. Sharma A, Matsuo S, Yang WL, Wang Z, Wang P. Receptor-interacting protein kinase 3 deficiency inhibits immune cell infiltration and attenuates organ injury in sepsis. *Crit Care*. 2014;18:R142.
15. Oerlemans MI, Liu J, Arslan F, den Ouden K, van Middelaar BJ, Doevendans PA, et al. Inhibition of RIP1-dependent necrosis prevents adverse cardiac remodeling after myocardial ischemia-reperfusion in vivo. *Basic Res Cardiol*. 2012;107:270.
16. Deng XX, Li SS, Sun FY. Necrostatin-1 prevents necroptosis in brains after ischemic stroke via inhibition of RIPK1-mediated RIPK3/MLKL signaling. *Aging Dis*. 2019;10:807-17.
17. Liu YR, Xu HM. Protective effect of necrostatin-1 on myocardial tissue in rats with acute myocardial infarction. *Genet Mol Res*. 2016;15(2):https://doi.org/10.4238/gmr.15027298.
18. Takemoto K, Hatano E, Iwaisako K, Takeiri M, Noma N, Ohmae S, et al. Necrostatin-1 protects against reactive oxygen species (ROS)-induced hepatotoxicity in acetaminophen-induced acute liver failure. *FEBS Open Bio*. 2014;4:777-87.
19. Linkermann A, Bräsen JH, De Zen F, Weinlich R, Schwendener RA, Green DR, et al. Dichotomy between RIP1- and RIP3-mediated necroptosis in tumor necrosis factor-α-induced shock. *Mol Med*. 2012;18:577-86.
20. Sun L, Wang H, Wang Z, He S, Chen S, Liao D, et al. Mixed lineage kinase domain-like protein mediates necrosis signaling downstream of RIP3 kinase. *Cell*. 2012;148:213-27.
21. Wang Y, Wang J, Wang H, Feng X, Tao Y, Yang J, et al. Necrosulfonamide attenuates spinal cord injury via necroptosis inhibition. *World Neurosurg*. 2018;114:e1186-91.
22. Dmitriev Y, Minasian S, Bayrasheva V, Demchenko E, Galagudza M. Novel necroptosis inhibitors (necrosulfonamide and necrostatin-1S) demonstrate therapeutic potential for myocardial ischemia-reperfusion injury. *J Am Coll Cardiol*. 2017;69(11 Suppl):2058.
23. Takahashi M, Chen-Yoshikawa TF, Saito M, Tanaka S, Miyamoto E, Ohata K, et al. Immersing lungs in hydrogen-rich saline attenuates lung ischaemia-reperfusion injury. *Eur J Cardiothorac Surg*. 2017;51:442-8.
24. Nishiyama K, Sugiyama M, Yamada H, Makino K, Ishihara S, Takaki T, et al. A new approach for analyzing an adhesive bacterial protein in the mouse gastrointestinal tract using optical tissue clearing. *Sci Rep*. 2019;9:4731.
25. Nishikawa S, Menju T, Takahashi K, Miyata R, Chen-Yoshikawa TF, Sonobe M, et al. Statins may have double-edged effects in patients with lung adenocarcinoma after lung resection. *Cancer Manag Res*. 2019;11:3419-32.
26. Dong W, Zhang M, Zhu Y, Chen Y, Zhao X, Li R, et al. Protective effect of NSA on intestinal epithelial cells in a necroptosis model. *Oncotarget*. 2017;8:86726-35.
27. Zhang J, Yang Y, He W, Sun L. Necrosome core machinery: MLKL. *Cell Mol Life Sci*. 2016;73:2153-63.
28. Zhou Y, Zhou B, Tu H, Tang Y, Xu C, Chen Y, et al. The degradation of mixed lineage kinase domain-like protein promotes neuroprotection after ischemic brain injury. *Oncotarget*. 2017;8:68393-401.
29. Choi ME, Price DR, Ryter SW, Choi AMK. Necroptosis: a crucial pathogenic mediator of human disease. *JCI Insight*. 2019;4:e128834.
30. Krysko DV, Agostinis P, Krysko O, Garg AD, Bachert C, Lambrecht BN, et al. Emerging role of damage-associated molecular patterns derived from mitochondria in inflammation. *Trends Immunol*. 2011;32:157-64.
31. Tait SW, Oberst A, Quarato G, Milasta S, Haller M, Wang R, et al. Widespread mitochondrial depletion via mitophagy does not compromise necroptosis. *Cell Rep*. 2013;5:878-85.
32. Vanden Berghe T, Kalai M, Denecker G, Meeus A, Saelens X, Vandenabeele P. Necrosis is associated with IL-6 production, but apoptosis is not. *Cell Signal*. 2006;18:328-35.
33. Martín-Sánchez F, Diamond C, Zeitler M, Gomez AI, Baroja-Mazo A, Bagnall J, et al. Inflammasome-dependent IL-1β release depends upon membrane permeabilisation. *Cell Death Differ*. 2016;23:1219-31.
34. Linkermann A, Bräsen JH, Himmerkus N, Liu S, Huber TB, Kunzendorf U, et al. Rip1 (receptor-interacting protein kinase 1) mediates necroptosis and contributes to renal ischemia/reperfusion injury. *Kidney Int*. 2012;81:751-61.

Key Words: ischemia-reperfusion injury, cell death, apoptosis, necrosis, necroptosis, necrosulfonamide, receptor-interacting protein kinase-1, receptor-interacting protein kinase-3, mixed lineage kinase domain-like protein